

DYNAMICAL TRANSITION THEORY OF HEXAGONAL PATTERN FORMATIONS

TAYLAN ŞENGÜL

ABSTRACT. The main goal of this paper is to understand the formation of hexagonal patterns from the dynamical transition theory point of view. We consider the transitions from a steady state of an abstract nonlinear dissipative system. To shed light on the formation of mixed mode patterns such as the hexagonal pattern, we consider the case where the linearized operator of the system has two critical real eigenvalues, at a critical value λ_c of a control parameter λ with associated eigenmodes having a roll and rectangular pattern. By using center manifold reduction, we obtain the reduced equations of the system near the critical transition value λ_c . By a thorough analysis of these equations, we fully characterize all possible transition scenarios when the coefficients of the quadratic part of the reduced equations do not vanish. We consider three problems, two variants of the 2D Swift-Hohenberg equation and the 3D surface tension driven convection, to demonstrate that all the main theoretical results we obtain here are indeed realizable.

1. INTRODUCTION: MAIN ASSUMPTIONS AND RESULTS

Transition phenomena is throughout all nonlinear sciences [23, 16, 14]. It shapes many physical, biological and social systems through instabilities. The formation of patterns in such systems, whether it be coatings of animals [24], convection cells in fluid systems [1] or crime patterns in cities [35], is intrinsically related to the transitions taking place in those systems. One of the tools to understand and classify the transition behavior is the dynamic transition theory [23]. The current work is an attempt to combine this theory with certain aspects of pattern formations and relies on some of the previous work in this direction [10, 33, 34, 20].

1.1. The setting and the main assumptions. We are interested in the transitions of a steady state solution of a general nonlinear dissipative system [37] on a Hilbert space X

$$(1) \quad \frac{du}{dt} = L_\lambda u + G_\lambda(u), \quad t > 0$$

where $u : [0, \infty) \mapsto X$ is the unknown function and $\lambda \in \mathbb{R}^1$ is a parameter. Here $L_\lambda : X_1 \rightarrow X$ is a linear operator where X_1 is another

Date: January 17, 2022.

Banach space with compact and dense inclusion $X_1 \subset X$ and G_λ is a nonlinear operator satisfying certain properties given later.

1.1.1. *The assumptions on the spectrum of the linear operator.* We will assume that the linear operator L_λ has a countably infinite set of eigenvalues

$$\{\beta_i(\lambda) \in \mathbb{C} : i \in \mathbb{N}\}$$

with a complete set of eigenvectors

$$\{f_i \in X_1, i = 1, 2, \dots\}$$

satisfying the following conditions on its spectrum, known as the **PES conditions**.

$$(2) \quad \begin{aligned} &\beta_1(\lambda), \beta_2(\lambda) \in \mathbb{R}, \\ &\beta(\lambda) := \beta_1(\lambda) = \beta_2(\lambda) \begin{cases} < 0 & \lambda < \lambda_c \\ = 0 & \lambda = \lambda_c \\ > 0 & \lambda > \lambda_c \end{cases} \\ &Re\beta_i < 0, \quad \forall i = 3, 4, \dots \end{aligned}$$

Much of the linear theory on stability and transitions involves establishing the PES conditions, see [2] for the classical fluid dynamics and [28] for the geophysical fluid dynamics.

1.1.2. *The assumptions on the physical space.* As the physical space, we assume a bounded spatial domain with at least two dimensions. We also distinguish between the eigenvectors f_i of the linear operator and a (possibly) distinct set of basis vectors

$$\{e_{i_1, i_2}^j \in X_1 : i_1, i_2, j \in \mathbb{N}\}$$

indexed by the wave indices i_1, i_2 spanning the two horizontal spatial dimensions and j is the index of the other directions which we usually suppress for ease of notation. Moreover, we assume that the first two critical modes have the spatial structure

$$(3) \quad f_1 \sim e_{j_1, j_2}, \quad f_2 \sim e_{k_1, 0},$$

for some non-negative integers j_1, j_2, k_1 . Even for 2D problems, the basis vectors $e_{i,j}$ are usually different from the basis vectors f_j of the linear operator. *For example*, in a scalar reaction diffusion type equation, the vectors $e_{i,j}$ are usually the eigenbasis of the Laplacian operator with the given boundary conditions, while for fluid problems, the vectors $e_{i,j}$ are the eigenbasis of the Stokes operator, as we consider in [Section 3.3](#).

As an example, if the spatial domain of interest is a rectangular domain $(0, L_1\pi) \times (0, L_2\pi) \times (0, 1)$ with Neumann boundary conditions in the horizontal directions, then the eigenmodes f_j are given by

$$f_j = \sum_{k=1}^{\infty} \hat{f}_k e_{j_1, j_2}^k(x, y, z)$$

where

$$(4) \quad e_{j_1, j_2}^j = \cos(j_1 x_1 / L_1) \cos(j_2 x_2 / L_2) w_j(z)$$

where j_1, j_2 are non-negative integers and w_j are basis functions satisfying the vertical boundary conditions.

Under the assumption (3), the eigenmode f_1 represents a rectangular (horizontal) pattern, and the eigenmode f_2 represents a roll pattern. Their linear combinations give rise to mixed patterns such as the hexagonal pattern, see Figure 1.

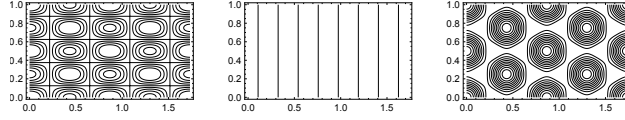


FIGURE 1. (a) A rectangular mode $\cos(\frac{4x_1}{\sqrt{3}}) \cos(4x_2)$
 (b) A roll mode $\cos(\frac{8x_1}{\sqrt{3}})$ (c) A mixed mode
 $4 \cos(\frac{4x_1}{\sqrt{3}}) \cos(4x_2) + \cos(\frac{8x_1}{\sqrt{3}})$.

In many physical examples, the critical modes are selected according to the horizontal wave number, that is the first two critical modes have equal horizontal wave numbers. This implies, (3) means

$$(5) \quad \left(\frac{j_1 \pi}{L_1}\right)^2 + \left(\frac{j_2 \pi}{L_2}\right)^2 = \left(\frac{k_1 \pi}{L_1}\right)^2$$

from which $k_1 > j_1$ follows. We remark here that, the equality of the wave numbers of the first two critical modes, imposes a severe relation on the horizontal aspect ratio L_2/L_1 of a rectangular domain.

$$(6) \quad L_1 = \sqrt{\frac{k_1^2 - j_1^2}{j_2^2}} L_2.$$

As a result, in applications, this type of transition is non-generic, that is, does not occur if the aspect ratio is chosen randomly. We give the choice of the wave indices for the 3D Rayleigh-Benard convection with free slip boundary conditions in Figure 2. The figure shows the non-genericity of the higher multiplicity transitions and the length scales at which double equal wave number mode transitions occur for (a) a roll and a rectangle mode, (b) two roll modes, (c) two rectangle modes.

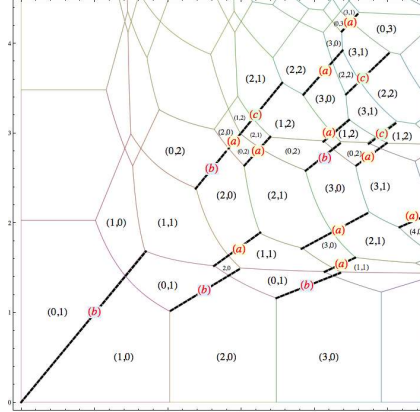


FIGURE 2. The critical index map for the 3D Rayleigh-Benard convection with respect to the horizontal length scales L_1 and L_2 , from [33].

1.1.3. *The main assumptions on the nonlinear operator.* We assume that G consists of higher order terms in u , that is $G_\lambda(u) = o(\|u\|_{X_\alpha})$ where X_α is an interpolation space with $0 \leq \alpha < 1$. This ensures that (1) admits the homogeneous steady state solution

$$u(t) = 0, \quad \forall t \geq 0.$$

We consider the following Taylor expansion of G .

$$(7) \quad G(u) = G_2(u, u) + G_3(u, u, u) + \dots$$

Here G_2 is the bilinear and G_3 is the trilinear operator of the Taylor expansion of G and the rest of the expansion will not play a role in the analysis.

The main assumption is the following orthogonality conditions on the bilinear G_2 and trilinear G_3 parts of the nonlinear operator with respect the basis vectors $e_{i,j}$. We assume that if $\pm i_r \pm j_r \neq \pm k_r$ for some choice of \pm and at least one of $r = 1, 2$ then

$$(8) \quad \langle G_2(e_{i_1, i_2}, e_{j_1, j_2}), e_{k_1, k_2} \rangle = 0.$$

Here $\langle \cdot \rangle$ represent the inner product of X . Similarly, $\pm i_r \pm j_r \pm k_r \neq \pm l_r$ for some choice of \pm and at least one of $r = 1, 2$, we assume that

$$(9) \quad \langle G_3(e_{i_1, i_2}, e_{j_1, j_2}, e_{k_1, k_3}), e_{l_1, l_2} \rangle = 0.$$

Such orthogonality conditions are typical for trigonometric basis functions and nonlinear operators which are products of functions and their derivatives. Our main assumptions are satisfied in many physically interesting systems such as the convective motions of fluids [17, 34, 33, 10, 11], reaction-diffusion systems [25, 19, 26, 42] and pattern formation equations [6, 41, 5]. We will also present several applications where these assumptions hold in Section 3.

For example for modes given by (4) and a general nonlinear operator of the form

$$G(u) = a_1 u^2 + a_2 u u_x + a_3 u u_y + a_4 u^3 + a_5 u^2 u_x + \dots$$

where a_i are constants and the usual L_2 inner product, the assertions hold true due to the orthogonality of trigonometric functions.

1.2. Discussion of the main results. We first derive the general structure of the reduced (amplitude) equations by using the center manifold reduction. Letting $u_1(t)f_1 + u_2(t)f_2$ to denote the center part of the solution, we obtain the following equations.

$$\begin{aligned} \frac{du_1}{dt} &= \beta(\lambda)u_1 + a_1 u_1 u_2 + u_1(a_2 u_1^2 + a_3 u_2^2) + O(4), \\ \frac{du_2}{dt} &= \beta(\lambda)u_2 + b_1 u_1^2 + u_2(b_2 u_1^2 + b_3 u_2^2) + O(4). \end{aligned}$$

These equations describe the long time behaviour of the system, near the transition point $\lambda = \lambda_c$ close to the basic steady state solution. The reduced equations consist of a quadratic part with coefficients a_1, b_1 due to the bilinear interactions between the critical modes and a cubic part with coefficients a_2, a_3, b_2 and b_3 due to the bilinear interactions of the critical modes with the higher frequency modes plus trilinear self interactions of the critical modes. Our analysis of the reduced equations shows that when none of the coefficients a_1, b_1, b_3 vanish, the type of transition depends only on these three parameters.

In this paper, we address the case $a_1 \neq 0, b_1 \neq 0$ and $b_3 \neq 0$. In the case $a_1 = b_1 = 0$, there are no bilinear interactions among the critical modes, and the behavior of the system is determined by the cubic coefficients a_2, a_3, b_2, b_3 . That case is generic case when the first two critical modes are both roll-type or both rectangle-type and is also often encountered in the applications [33]. It also occurs under certain symmetry conditions which frequently arise in nonlinear systems of interest. We will address this case in a future study.

Next, by a detailed analysis of the reduced equations, we describe the bifurcated steady states and their stability and describe all the possible transition scenarios. Due to the interactions of these two modes, a variety of new states emerge after transition, including those associated with hexagonal patterns.

In terms of transition analysis, our guiding principle is the dynamic transition theory of Ma and Wang [23]. The key philosophy of dynamic transition theory is to search for the full set of transition states, giving a complete characterization of stability and transition. The set of transition states is a local attractor, representing the physical reality after the transition. As a general principle, dynamic transitions of all dissipative systems are classified into three categories: *continuous (Type-I)*,

catastrophic (Type-II), and random (Type-III). Intuitively, a continuous transition occurs when the system transitions to a nearby local attractor, a catastrophic transition occurs when there are no nearby local attractors after transition and finally random transition occurs when the system either moves to a local attractor or leave the local neighborhood depending on the initial perturbation. For some of the recent applications of this theory, we refer to [39, 40, 21, 15, 12].

Our analysis shows that four different transitions are possible depending on the signs of a_1b_1 and b_3 . When $a_1b_1 > 0$ there are always bifurcated saddle mixed mode steady states near the basic solution on both sides of $\lambda = \lambda_c$. Moreover, the transition is either catastrophic or random depending on the sign of b_3 . In the catastrophic transition, there are no steady states bifurcated from the basic solution after the transition $\lambda > \lambda_c$ and a repeller bifurcates on $\lambda < \lambda_c$. In the random transition scenario, the evolution of the system depends on the fluctuations (initial conditions) of the basic solution. Namely, the phase space separates into two sectorial regions where solutions starting from the first region leave the neighbourhood of the basic solution and solutions starting from the second region tend to an attractor nearby which consists of three steady states and the orbits between them.

When $a_1b_1 < 0$, the only bifurcated steady states are the two roll-type solutions which are symmetric of each other. Depending on the sign of b_3 , there is either a continuous transition or a catastrophic transition. In the continuous transition case, the two roll type solutions are bifurcated on $\lambda > \lambda_c$ with one being stable and the other being saddle. In this case, there is an S^1 attractor which consists of these two steady states and the heteroclinic orbits connecting them. In the catastrophic transition case, there are no steady states bifurcated on $\lambda > \lambda_c$ and two roll type solutions are bifurcated on $\lambda < \lambda_c$ which form a repeller homeomorphic to S^1 .

After the presentation of the general theory, we give three applications which show that all the transitions described by our main theorems are indeed observable. We consider two variants of the 2D Swift Hohenberg equation with quadratic-cubic nonlinearity. The last application is the 3D surface tension driven convection also known as Marangoni convection. For both systems, we demonstrate that our main assumptions are satisfied and describe the transition behavior from the main results we have proved.

1.3. Notations. We denote the adjoint eigenvectors by f_j^* which are found by

$$L^* f_j^* = \overline{\beta_j} f_j^*,$$

where L^* is the adjoint linear operator. The eigenvectors of the linear and adjoint operator satisfy the orthogonality property

$$\langle f_j, f_k^* \rangle = \delta_{jk} \langle f_j, f_j^* \rangle.$$

with $\langle \cdot, \cdot \rangle$ denoting the inner product in X .

Recalling G_2 and G_3 from (7), for ease of notation, we will denote the bilinear and trilinear interactions of modes by

$$(10) \quad \begin{aligned} G_2(i, j, k) &= \frac{1}{\langle f_k, f_k^* \rangle} \langle G_2(f_i, f_j), f_k^* \rangle \\ G_2^s(i, j, k) &= G_2(i, j, k) + G_2(i, k, j) \end{aligned}$$

Similarly for the trilinear operator,

$$(11) \quad \begin{aligned} G_3(i, j, k, l) &= \frac{1}{\langle f_l, f_l^* \rangle} \langle G_3(f_i, f_j, f_k), f_l^* \rangle \\ G_3^s(i, j, k, l) &= \sum_{\sigma} G_3(\sigma(i, j, k), l) \end{aligned}$$

where the summation is over all permutations σ of the triple (i, j, k) .

2. MAIN TRANSITION THEOREMS

In this section, we present the main results on transitions of the system (1) under the given conditions. According to dynamic transition theory, in any dissipative system, there are only three possible transition types. The intuitive understanding of three types of transitions is mentioned in the Introduction. For the exact definitions of three types of transitions we refer to [23].

2.1. The reduced equations. We first give the reduced equations with the exact expressions for their coefficients and mention several remarks regarding these equations.

We denote the center part of the solution spanned by the first two critical modes by

$$u_c = u_1(t)f_1 + u_2(t)f_2$$

where f_1 and f_2 given by (3) are the first critical modes satisfying the PES conditions (2) and $u_1(t), u_2(t) \in \mathbb{R}$ are the time dependent amplitudes of these modes.

In Section 4, we prove that the dynamics of near the system near the origin and close to onset of transition $\lambda = \lambda_c$ is given by the following reduced equations become

$$(12) \quad \begin{aligned} \frac{du_1}{dt} &= \beta(\lambda)u_1 + F_1(x) + O(4) \\ \frac{du_2}{dt} &= \beta(\lambda)u_2 + F_2(x) + O(4) \end{aligned}$$

where the vector field $F = (F_1, F_2)$ is defined as follows:

$$(13) \quad \begin{aligned} F_1(u_1, u_2) &= a_1 u_1 u_2 + u_1 (a_2 u_1^2 + a_3 u_2^2), \\ F_2(u_1, u_2) &= b_1 u_1^2 + u_2 (b_2 u_1^2 + b_3 u_2^2) \end{aligned}$$

and

$$O(n) = O(|x|^n) + O(|x|^{n-1}\beta(\lambda)), \quad \text{as } x \rightarrow 0, \lambda \rightarrow \lambda_c.$$

Here the coefficients of the quadratic terms are

$$(14) \quad \begin{aligned} a_1 &= G_2^s(1, 2, 1) \\ b_1 &= G_2(1, 1, 2) \end{aligned}$$

and the coefficients of the cubic terms are

$$(15) \quad \begin{aligned} a_2 &= G_3(1, 1, 1, 1) + \sum_{j \geq 3} \frac{-1}{\beta_j} G_2(1, 1, j) G_2^s(1, j, 1) \\ a_3 &= G_3^s(1, 2, 2, 1) + \sum_{j \geq 3} \frac{-1}{\beta_j} \left(G_2(1, 2, j) G_2^s(2, j, 1) \right. \\ &\quad \left. + G_2(2, 1, j) G_2^s(2, j, 1) + G_2(2, 2, j) G_2^s(1, j, 1) \right) \\ b_2 &= G_3^s(1, 1, 2, 2) + \sum_{j \geq 3} \frac{-1}{\beta_j} \left(G_2(1, 1, j) G_2^s(2, j, 2) \right. \\ &\quad \left. + G_2(1, 2, j) G_2^s(1, j, 2) + G_2(2, 1, j) G_2^s(1, j, 2) \right) \\ b_3 &= G_3(2, 2, 2, 2) + \sum_{j \geq 3} \frac{-1}{\beta_j} G_2(2, 2, j) G_2^s(2, j, 2) \end{aligned}$$

Remarks.

- (1) We note that the cubic terms depend on the interactions of the first two modes with higher modes (f_j with $j \geq 3$), while the quadratic terms are determined solely by the self-interactions of the first two modes.
- (2) The reduced equations (12) are symmetric under $u_1 \mapsto -u_1$. As a result, the reduced phase portrait is symmetric with respect to u_2 axis.
- (3) The first equation of the reduced equation can be solved as

$$u_1(t) = u_1(0) \exp \left(\int_0^t (a_1 u_2(s) + a_2 u_1^2(s) + a_3 u_2^2(s)) ds \right)$$

As a result, in the reduced phase portrait, the sign of $u_1(0)$ is preserved by $u_1(t)$.

- (4) When the first two modes are both rolls or both rectangles with equal wave numbers, our analysis can be extended to show that quadratic part of the reduced equations vanish while the cubic part remains the same. However, our main theorems only deal with the case of non-vanishing quadratic terms a_1 and b_1 . We plan to address the case $a_1 = b_1 = 0$ later.
- (5) In this paper, we will always assume that $b_3 \neq 0$. Otherwise, $(0, 0)$ can easily be seen to be non-isolated singular point of F .

- (6) When the critical modes have equal horizontal wave numbers as discussed in 1.1, we have the relation $k_1 > j_1$ between the wave indices in (3). In that case, $C_{11} \cap C_{22} = \emptyset$ and the $G_2(2, 2, j)G_2^s(1, j, 1)$ term in a_3 and $G_2(1, 1, j)G_2^s(2, j, 2)$ in b_2 also vanish as a result.

Moreover, when the wave numbers of the critical modes are equal, in the sums (15), only modes f_j spanned by e_{ik} with wave indices (i, k) in C_{11} for a_2 , C_{12} for a_3 , b_2 and C_{22} for b_3 have to be considered where

$$(16) \quad \begin{aligned} C_{11} &= \{(2j_1, 2j_2), (2j_1, 0), (0, 2j_2)\}, \\ C_{12} &= \{(k_1 - j_1, j_2), (k_1 + j_1, j_2)\}, \\ C_{22} &= \{(2k_1, 0)\}. \end{aligned}$$

- (7) The quadratic part of the reduced equations is degenerate and as a result, to study the transition behaviour, the cubic part (only b_3 term, as we shall see) is also necessary.

2.2. The statement of the main theorems. Before we state the main theorems, we briefly discuss the possible bifurcated steady state solutions of the system (1) and give the conditions which dictate their existence and stability.

$$(17) \quad \begin{aligned} R_1 &= -\sqrt{-\frac{\beta}{b_3}}f_2 + o(\sqrt{-\beta}), \\ R_2 &= \sqrt{-\frac{\beta}{b_3}}f_2 + o(\sqrt{-\beta}) \end{aligned}$$

and

$$(18) \quad \begin{aligned} H_1 &= \frac{1}{\sqrt{a_1 b_1}}\beta f_1 - \frac{1}{a_1}\beta f_2 + o(\beta), \\ H_2 &= -\frac{1}{\sqrt{a_1 b_1}}\beta f_1 - \frac{1}{a_1}\beta f_2 + o(\beta), \end{aligned}$$

where f_1, f_2 are the first critical eigenmodes with eigenvalue β satisfying the PES conditions given by (2). First, we note the scale difference between the steady states $R_i = O(-\sqrt{\beta})$ and $H_i = O(\beta)$ as $\beta \rightarrow 0$. Thus the steady states H_i are much closer to the basic steady state than R_i . Second R_i denote the bifurcated solutions which have the spatial roll pattern $e_{k_1, 0}$ plus small perturbations when the eigenmodes are given by (3). These solutions are defined only when $\beta(\lambda)b_3 < 0$. Third, H_i denote the mixed mode bifurcated steady state solutions which may spatially represent hexagonal patterns. These solutions are defined when $a_1 b_1 > 0$.

As is well known the transitions of the system are captured by the reduced equations (12) which contains 6 coefficients determined by the system. In the case $a_1 \neq 0, b_1 \neq 0$, the critical modes have self interactions. In addition, if $b_3 \neq 0$, we will show that the transition of the

system depends only on the signs of the 3 out of 6 coefficients a_1 , b_1 and b_3 in (12). In this case, the remaining coefficients a_2 , a_3 and b_2 play a quantitative but not a qualitative role. Our main theorems classify the transitions depending on the signs of these three coefficients as well as the stability of the above steady states. We summarize this in Table 1 and Table 2.

$a_1 b_1$	b_3	Theorem	Transition Type	Transition Diagram
> 0	< 0	Theorem 2.1(i)	random	Figure 3
> 0	> 0	Theorem 2.1(ii)	catastrophic	Figure 4
< 0	< 0	Theorem 2.2(i)	continuous	Figure 5
< 0	> 0	Theorem 2.1(ii)	catastrophic	Figure 6

TABLE 1. The type of transition and the conditions required.

$a_1 b_1$	b_3	H_i on $\lambda \neq \lambda_c$	R_i on $\lambda < \lambda_c$	R_i on $\lambda > \lambda_c$
> 0	< 0	both are SAD	DNE	R_1 is a SN, R_2 is a SAD
> 0	> 0	both are SAD	R_1 is a SAD, R_2 is an UN	DNE
< 0	< 0	DNE	DNE	R_1 is a SN, R_2 is a SAD
< 0	> 0	DNE	R_1 is a SAD, R_2 is an UN	DNE

TABLE 2. Stability properties of the bifurcated steady states for $a_1 > 0$. For $a_1 < 0$, the stability of H_i is unchanged while the stability of R_1 and R_2 is exchanged. Here SAD = saddle, SN = stable node, UN = unstable node, DNE = does not exist.

Under the conditions given in Section 1.1, the transition behavior of the general dissipative system (1) is given by the following two theorems.

Theorem 2.1. *Assume $a_1 b_1 > 0$.*

- i) If $b_3 < 0$ then the system (1) undergoes a random (Type-III) transition at $\lambda = \lambda_c$ described as below.*

a) The topological structure of the transition is as in [Figure 3](#).

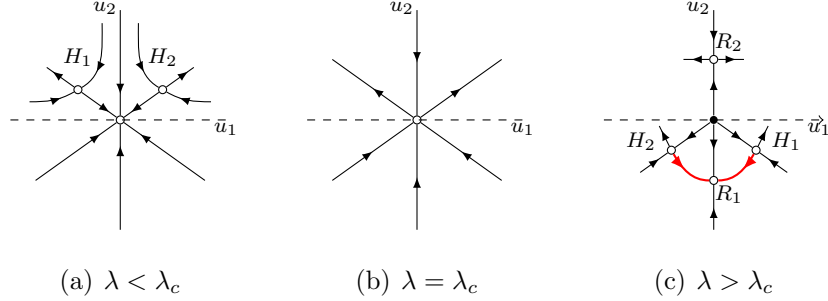


FIGURE 3. The structure of the transition for $a_1 b_1 > 0$, $b_3 < 0$, $a_1 > 0$. The bifurcated attractor Σ_λ on $\lambda > \lambda_c$ is shown in red. When $a_1 < 0$, the assertions given by [Theorem 2.1](#) hold true with the regions and the steady states flipped with respect to the u_1 axis.

b) There is a neighborhood \mathcal{U} of $\phi = 0$ in the phase space X such that for any $\lambda_c < \lambda < \lambda_c + \epsilon$ with some $\epsilon > 0$, \mathcal{U} can be decomposed into two open sets $\mathcal{U}_1^\lambda, \mathcal{U}_2^\lambda$,

$$\overline{\mathcal{U}} = \overline{\mathcal{U}_1^\lambda} \cup \overline{\mathcal{U}_2^\lambda}, \quad \mathcal{U}_1^\lambda \cap \mathcal{U}_2^\lambda = \emptyset$$

such that

$$\begin{aligned} \lim_{\lambda \rightarrow \lambda_c} \limsup_{t \rightarrow \infty} \|S_\lambda(t, \varphi)\|_X &= 0 & \forall \varphi \in \mathcal{U}_1^\lambda, \\ \limsup_{t \rightarrow \infty} \|S_\lambda(t, \varphi)\|_X &\geq \delta > 0 & \forall \varphi \in \mathcal{U}_2^\lambda, \end{aligned}$$

for some $\delta > 0$. Here S_λ is the evolution of the solution with initial data φ . Moreover $\mathcal{P}(U_1^\lambda), \mathcal{P}(U_2^\lambda)$ are sectorial regions as shown in [Figure 3\(c\)](#) with angles $\pi - 2\theta$ and $\pi + 2\theta$ respectively, where $\theta = \arctan \sqrt{a_1/b_1}$ and \mathcal{P} is the projection onto the plane spanned by f_1, f_2 .

c) The system bifurcates to an attractor Σ_λ which consists of three steady states R_1, H_1, H_2 and the heteroclinic orbits connecting H_i to $R_1, i = 1, 2$. Namely, Σ_λ is the arc connecting these three steady states as shown in [Figure 3\(c\)](#), and has \mathcal{U}_1^λ as its basin of attraction.

ii) If $b_3 > 0$ then the system undergoes a catastrophic (Type-II) transition at $\lambda = \lambda_c$ and the following assertions are true:

a) The topological structure of the transition is as given by [Figure 4](#).

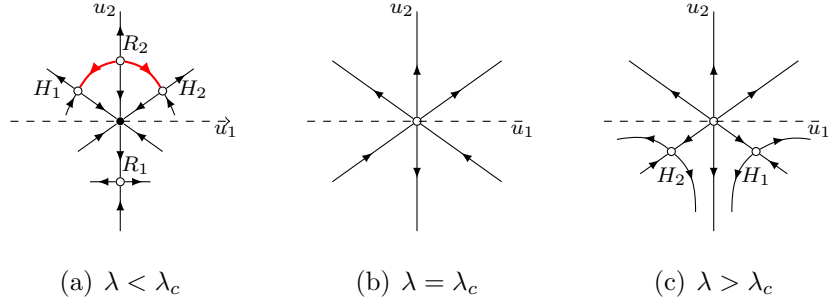


FIGURE 4. The structure of transition for $a_1 b_1 > 0$, $b_3 > 0$, $a_1 > 0$. The bifurcated repeller Σ_λ on $\lambda < \lambda_c$ is shown in red color. For $a_1 < 0$, the same transition diagram is obtained with H_1 , H_2 solutions reflected along u_1 axis for $\lambda > \lambda_c$.

- b) There is a bifurcated repeller Σ_λ on $\lambda < \lambda_c$ which consists of three steady states, H_1, H_2, R_2 and the heteroclinic orbits connecting R_2 to H_1 and H_2 respectively. Σ_λ , topologically.
- c) Finally for $\lambda_c + \epsilon > \lambda > \lambda_c$ there is an open neighborhood \mathcal{U} of $\phi = 0$ and a dense, open subset \mathcal{U}^λ of \mathcal{U} such that

$$\limsup_{t \rightarrow \infty} \|S_\lambda(t, \varphi)\|_X \geq \delta > 0, \quad \forall \varphi \in \mathcal{U}^\lambda,$$

for some $\delta > 0$.

Theorem 2.2. Assume $a_1 b_1 < 0$.

- i) If $b_3 < 0$, then the system (1) undergoes a continuous (Type-I) transition at $\lambda = \lambda_c$ described as below.
- a) The topological structure is as given by [Figure 5](#).

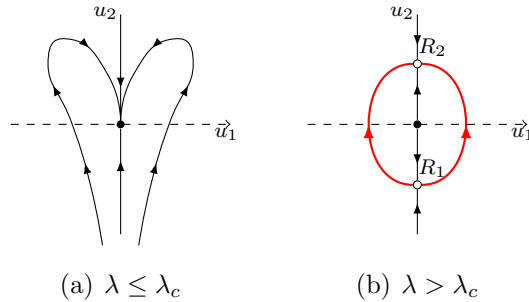


FIGURE 5. The structure of transition for $a_1 b_1 < 0$, $b_3 < 0$.

- b) The system bifurcates on $\lambda > \lambda_c$ to an attractor Σ_λ which is homeomorphic to S^1 . Σ_λ consists of two singular points R_i , $i = 1, 2$ and two heteroclinic orbits connecting them. Moreover there exists a neighborhood \mathcal{U}^λ of $\phi = 0$ such

that Σ_λ attracts $\mathcal{U}^\lambda \setminus \Gamma$ where Γ is the stable manifold of $\phi = 0$ with $\text{codim}\Gamma = 2$.

ii) If $b_3 > 0$, then the system undergoes a catastrophic (Type-I) transition at $\lambda = \lambda_c$.

a) The topological structure is as given by [Figure 6](#).

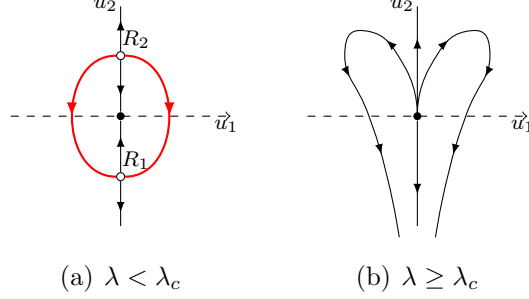


FIGURE 6. The structure of transition for $a_1 b_1 < 0, b_3 > 0$.

b) The system bifurcates to a repeller Σ_λ on $\lambda < \lambda_c$ which consists of two critical points $R_i, i = 1, 2$ and heteroclinic orbits connecting them.

3. APPLICATIONS

In this section, we give several applications to demonstrate that all the results obtained in our main theorems are indeed realizable.

3.1. 2D Swift-Hohenberg Equation with quadratic-cubic nonlinearity. We first consider the 2D Swift-Hohenberg equation

$$(19) \quad u_t = \lambda u - (\Delta + k)^2 u + \alpha_2 u^2 - \alpha_3 u^3$$

with $\alpha_2, \alpha_3, k, \lambda \in \mathbb{R}$ and $u = u(x, y, t)$ is the unknown function. The Swift-Hohenberg equation (SHE) was first proposed in 1977 [36] as a simple model for the Rayleigh-Benard instability of roll waves. For previous results on instabilities and physical aspects of the model, we refer to [29, 3, 18, 13]

We consider a spatial domain

$$(20) \quad \Omega = (0, \sqrt{3}\pi) \times (0, \pi),$$

and Neumann boundary conditions

$$(21) \quad \frac{\partial u}{\partial \nu} = \frac{\partial \Delta u}{\partial \nu} = 0 \quad \text{on } \partial\Omega,$$

where ν is the unit outward normal to $\partial\Omega$. We also assume zero mean conditions

$$(22) \quad \iint_{\Omega} u dx dy = 0.$$

For the functional setting, let

$$(23) \quad \begin{aligned} H &= \{u \in L^2(\Omega) \mid \int_{\Omega} u \, dx = 0\}, \\ H_1 &= \{u \in H^4(\Omega) \cap H \mid u \text{ satisfies (21) and (22)}\}. \end{aligned}$$

Let $L_{\lambda} : H_1 \rightarrow H$ and $G : H_1 \rightarrow H$ be defined by

$$(24) \quad \begin{aligned} L_{\lambda}u &= \lambda u - (\Delta + k)^2u, \\ G(u) &= \alpha_2u^2 - \alpha_3u^3. \end{aligned}$$

Then the problem (19) with (21) can be written as

$$(25) \quad \begin{aligned} \frac{du}{dt} &= L_{\lambda}u + G(u), \\ u(0) &= u_0. \end{aligned}$$

Under these conditions, the eigenvalue problem

$$\lambda u - (\Delta + k)^2u = \beta u$$

has eigenfunctions

$$e_{j_1, j_2}(x, y) = \cos(j_1 \frac{x}{\sqrt{3}}) \cos(j_2 y)$$

and eigenvalues

$$\beta_{j_1, j_2} = \lambda - (k - |J|^2)^2, \quad J = (j_1, j_2) \in \mathcal{J}$$

Here

$$|(j_1, j_2)|^2 = \frac{j_1^2}{3} + j_2^2$$

$$\mathcal{J} = \{(j_1, j_2) \in \mathbb{Z}_{\geq 0} \times \mathbb{Z}_{\geq 0} : (j_1, j_2) \neq (0, 0)\}$$

It is easy to see that the PES condition is satisfied with

$$\lambda_c(k) = \min_{J \in \mathcal{J}} (k - |J|^2)^2 = (k - |J_i|^2)^2, \quad i = 1, \dots, n$$

The minimum occurs at $|J|^2 = k$ when $k \in \mathcal{J}$. If $k \notin \mathcal{J}$, then it occurs at one of $k_1, k_2 \in \mathcal{J}$ for which $k_1 < k < k_2$. Note that

$$|(1, 0)| < |(0, 1)| < |(1, 1)| = |(2, 0)| < |(2, 1)| < \dots$$

Thus solving $(k - |J|^2)^2 = (k - |\tilde{J}|^2)^2$ for k for the first two consecutive $|J|, |\tilde{J}|$ gives the following result.

$$\begin{cases} J_1 = (1, 0) & \text{if } 0 < k \leq 4/6 \\ J_1 = (0, 1) & \text{if } 4/6 \leq k \leq 7/6 \\ J_1 = (1, 1), J_2 = (2, 0) & \text{if } 7/6 \leq k \leq 11/6 \\ J_1 = (2, 1) & \text{if } 11/6 \leq k < 19/6 \end{cases}$$

In particular, note that when

$$(26) \quad 7/6 < k < 11/6, \quad \lambda_c = (k - 4/3)^2,$$

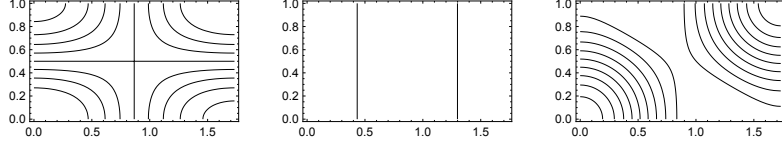


FIGURE 7. The bifurcated solutions.

there are two critical modes

$$f_1 = e_{1,1} = \cos \frac{x}{\sqrt{3}} \cos y, \quad f_2 = e_{2,0} = \cos \frac{2x}{\sqrt{3}},$$

with corresponding eigenvalues satisfying the PES condition

$$(27) \quad \beta_{1,1} = \beta_{2,0} = \lambda - \lambda_c \begin{cases} < 0, & \lambda < \lambda_c \\ = 0, & \lambda = \lambda_c \\ > 0, & \lambda > \lambda_c \end{cases}$$

$$\beta_{j_1, j_2} < 0, \quad (j_1, j_2) \notin \{(1, 1), (2, 0)\}.$$

Thus the main assumptions are all satisfied. Hence, the PDE system can be reduced to the ODE system (12) near $\lambda = \lambda_c$ and for small (u_1, u_2) where u_1, u_2 are the time dependent amplitudes of the modes f_1, f_2 .

Now we can compute the coefficients (14), (15) that determines the type of transition. We let

$$G_2(i, j, k) = \alpha_2 \int_{\Omega} f_i f_j f_k dx dy$$

$$G_3(i, j, k, l) = \alpha_3 \int_{\Omega} f_i f_j f_k f_l dx dy$$

Hence

$$a_1 = \alpha_2, \quad b_1 = \frac{\alpha_2}{4}, \quad b_3 = \frac{3(\alpha_2^2 + 4(3k - 10)\alpha_3)}{(160 - 48k)}.$$

Note that $a_1 b_1 \geq 0$. Also if $\alpha_2 \neq 0$ then necessarily $a_1 b_1 > 0$. For the range of k values we are interested, $7/6 < k < 11/6$,

$$b_3 \sim \alpha_2^2 + 4(3k - 10)\alpha_3$$

and $b_3 > 0$ if $\alpha_3 < 0$ and can be of both signs when $\alpha_3 > 0$.

Theorem 3.1. *Under the conditions (26) and $\alpha_2 \neq 0$, the basic solution $u = 0$ of the equation (25) undergoes a transition at $\lambda = \lambda_c$. The type of transition is either continuous if $b_3 < 0$ or catastrophic if $b_3 > 0$ as described by Theorem 2.1. In particular, if $\alpha_3 \leq 0$ then $b_3 > 0$, while for $\alpha_3 > 0$, depending on α_2 , b_3 can be of both signs, where α_2 and α_3 are the coefficients of the bilinear and trilinear terms in (19). The structure of the bifurcated mixed modes are as given in Figure 7.*

3.2. Modified 2D Swift Hohenberg Equation. We will now show that both transition scenarios described by [Theorem 2.2](#) are possible. For this let us consider the following equation which is more general than [\(19\)](#).

$$(28) \quad u_t = \lambda u - (\Delta + k)^2 u + G(u, u) - \alpha_3 u^3$$

where the bilinear operator is

$$(29) \quad G(u, v) = (c_1 + c_2 u_x + c_3 u_y)v + u(c_4 v_x + c_5 v_y)$$

on the rectangular domain [\(20\)](#) with the following boundary conditions

$$(30) \quad \begin{aligned} u = \Delta u = 0, & \quad x = 0, \sqrt{3}\pi, \\ u_y = \Delta u_y = 0, & \quad y = 0, \pi. \end{aligned}$$

This time, the basis functions are

$$e_{j_1, j_2}(x, y) = \sin(j_1 \frac{x}{\sqrt{3}}) \cos(j_2 y)$$

$$(31) \quad 5/6 < k < 11/6, \quad \lambda_c = (k - 4/3)^2,$$

and there are two critical modes

$$f_1 = e_{1,1} = \sin \frac{x}{\sqrt{3}} \cos y, \quad f_2 = e_{2,0} = \sin \frac{2x}{\sqrt{3}},$$

with corresponding eigenvalues satisfying the PES condition [\(27\)](#). In this case, the numbers describing the transition are found to be

$$a_1 = -\frac{(c_2 + c_4)^2}{2\sqrt{3}}, \quad b_1 = \frac{c_2 + c_4}{4\sqrt{3}}, \quad b_3 = \frac{(c_2 + c_4)^2 + 6(10 - 3k)\alpha_3}{24k - 80}$$

It is readily seen that for $c_2 + c_4 \neq 0$, $a_1 b_1 < 0$ and the transition is described by the following theorem.

Theorem 3.2. *Under the conditions [\(31\)](#) and $c_2 + c_4 \neq 0$, the basic solution $u = 0$ of the equation [\(28\)](#) with [\(30\)](#) undergoes a transition at $\lambda = \lambda_c$. The type of transition is either continuous if $b_3 < 0$ or catastrophic if $b_3 > 0$ as described by [Theorem 2.2](#). In particular, if $\alpha_3 \geq 0$ then $b_3 < 0$, while for $\alpha_3 < 0$, depending on $c_2 + c_4$, b_3 can be of both signs, where c_2 , c_4 and α_3 are the coefficients of the bilinear and trilinear terms in [\(28\)](#).*

3.3. Surface tension driven convection. In this section, we present known results on the hexagonal pattern formation in surface tension driven convection also known as Marangoni convection to show that it fits into the framework we present in this study. The nondimensional form of the equations describing the Marangoni convection without

gravity are, [8, 38],

$$(32) \quad \begin{aligned} \frac{\partial \mathbf{u}}{\partial t} + (\mathbf{u} \cdot \nabla) \mathbf{u} &= \text{Pr}(-\nabla p + \Delta \mathbf{u}), \\ \frac{\partial \theta}{\partial t} + (\mathbf{u} \cdot \nabla) \theta &= w + \Delta \theta, \\ \nabla \cdot \mathbf{u} &= 0. \end{aligned}$$

For the physical description and results about previous results on the instabilities of the above system, we refer to [27, 30, 31, 8, 7, 9, 4, 10]. Here $\mathbf{u} = (u, v, w)$ is the velocity field, T is the temperature, p is the pressure, $\text{Pr} = \nu/\kappa > 0$ is the Prandtl number. The unknowns represent a deviation from the motionless basic solution with a linear temperature profile given by,

$$\begin{aligned} \mathbf{u}_b &= 0, \\ T_b &= T_0 + (T_1 - T_0)z, \\ p_b(z) &= p_0 + g\rho_0(z - \alpha(T_1 - T_0)z^2/2), \end{aligned}$$

where T_0, T_1 are the temperatures at $z = 0$ and $z = 1$ respectively.

We consider the equations (1) on a rectangular domain

$$\Omega = (0, L_1) \times (0, L_2) \times (0, 1) \subset \mathbb{R}^3.$$

We supplement the above system with free-slip boundary conditions on the lateral boundaries, and the rigid (no slip) boundary condition and perfectly conducting on the bottom boundary. The top surface is assumed to be a non-deformable free surface with a surface tension of the form

$$\xi = \xi_0(1 - \gamma_T \theta).$$

Namely, the boundary conditions are as follows:

$$(33) \quad \begin{aligned} u = \frac{\partial v}{\partial x} = \frac{\partial w}{\partial x} = \frac{\partial \theta}{\partial x} &= 0 && \text{at } x = 0, L_1, \\ \frac{\partial u}{\partial y} = v = \frac{\partial w}{\partial y} = \frac{\partial \theta}{\partial y} &= 0 && \text{at } y = 0, L_2, \\ u = v = w = \theta &= 0 && \text{at } z = 0, \\ \frac{\partial(u, v)}{\partial z} + \lambda \nabla_H \theta = w = \frac{\partial \theta}{\partial z} + \text{Bi} \theta &= 0 && \text{at } z = 1, \end{aligned}$$

where $\nabla_H = (\partial_x, \partial_y)$, $\text{Bi} \geq 0$ is the Biot number, and the Marangoni number λ is the control parameter which represents the ratio of the destabilizing surface tension gradient to the stabilizing forces associated with thermal and viscous diffusion.

By the separation of variables, we represent the solutions in the following form:

$$(34) \quad \begin{aligned} u_I &= U_I(z) \sin L_1^{-1} I_x \pi x \cos L_2^{-1} I_y \pi y, \\ v_I &= V_I(z) \cos L_1^{-1} I_x \pi x \sin L_2^{-1} I_y \pi y, \\ w_I &= W_I(z) \cos L_1^{-1} I_x \pi x \cos L_2^{-1} I_y \pi y, \\ \theta_I &= \Theta_I(z) \cos L_1^{-1} I_x \pi x \cos L_2^{-1} I_y \pi y, \end{aligned}$$

for $I = (I_x, I_y) \in \mathbb{Z} \times \mathbb{Z}$. If instead of free-slip boundaries, no-slip boundaries are considered then the corresponding eigenvalue problem has to be solved by numerical methods [7, 32].

In [10], the following are proved:

- (1) When the relation (6) between the horizontal length scales of the domain is satisfied, it is possible that two modes with indices (j_1, j_2) and $(0, 2j_2)$ are the first two critical modes satisfying the PES condition (2) at the critical Marangoni number λ_c , introduced in [27] is defined as

$$\lambda_c = \min_{\alpha} \frac{8\alpha (\alpha \cosh \alpha + \text{Bi} \sinh \alpha) (\alpha - \cosh \alpha \sinh \alpha)}{\alpha^3 \cosh \alpha - \sinh^3 \alpha},$$

where the minimum is taken over wave numbers

$$\alpha = \alpha_{j,k} = ((L_1^{-1} j)^2 + (L_2^{-1} k))^2 \pi.$$

The map of critical index selection is similar to (2).

- (2) Under the above setting, the system has a transition described by the reduced equations (12). Moreover the coefficients of the reduced equations satisfy

$$a_1 = 4b_1, \quad a_3 = 2b_3, \quad 4a_2 = a_3 + b_2$$

- (3) Thus $a_1 b_1 > 0$ and the transition is as described by [Theorem 2.1](#). The sign of b_3 is found to be negative in a limited parameter space and thus the transition is found to be random (Type-III).

4. PROOFS

In this section, we give the proofs of our main theorems. Our strategy is first to obtain the reduction onto the center manifold of the dynamics and second, to analyze the reduced equations.

4.1. Center manifold approximation. We recall that the center part of the solution is given by

$$u_c = u_1(t) f_1 + u_2(t) f_2$$

The rest of the solution is approximated by the center manifold which we expand as

$$(35) \quad \Phi = \sum_{k \geq 3} \Phi_k(t) f_k$$

As is well known, see [23], the lowest order (quadratic) approximation of Φ is obtained as the solution of

$$(36) \quad \mathcal{L}\Phi = -P_s G(u_c) + o(2).$$

Here $P_s : X \rightarrow E_s$ is the projection operator where E_s is the stable space which is the span of $\{f_j : j \geq 3\}$ in X and $\mathcal{L} = L|_{E_s}$ is the restriction of the linear operator onto the stable space.

Since $f_j \in E_s$, for $j \geq 3$, we have

$$(37) \quad \langle P_s(\cdot), f_j^* \rangle = \langle \cdot, f_j^* \rangle, \quad j \geq 3.$$

Plugging (35) in (36), taking the inner product of (36) with f_j , $j \geq 3$ and making use of (37), we get

$$(38) \quad \Phi_j \beta_j \langle f_j, f_j^* \rangle = \langle \Phi, L^* f_j \rangle = -\langle G(u_c), f_j^* \rangle, \quad j \geq 3.$$

From (38), using the notation (10), we obtain the below formula for the coefficients of the center manifold.

$$(39) \quad \begin{aligned} \Phi_j &= \frac{-1}{\beta_j \langle f_j, f_j^* \rangle} \langle G(u_c), f_j^* \rangle \\ &= \frac{-1}{\beta_j} \sum_{m,n=1,2} u_m u_n G_2(m, n, j), \quad j \geq 3. \end{aligned}$$

Notice that Φ_j is independent of the trilinear operator G_3 .

Now the reduced equations of the system are obtained by plugging

$$u = u_c + \Phi$$

into the main equation (1), which is basically considering the dynamics on the center manifold and taking projection onto the center space, that is the span of the $\{f_1, f_2\}$. This gives

$$\frac{d}{dt} \langle u, f_k^* \rangle = \langle L_\lambda u, f_k^* \rangle + \langle G_\lambda(u), f_k^* \rangle, \quad k = 1, 2,$$

which is equivalent to the system

$$(40) \quad \frac{du_k}{dt} = \beta_k u_k + \frac{1}{\langle f_k, f_k^* \rangle} \langle G(u_c + \Phi), f_k^* \rangle, \quad k = 1, 2.$$

To obtain a closed system, we have to write the nonlinear term above as a function of u_1, u_2 . This can be obtained as follows

$$\begin{aligned} & \frac{1}{\langle f_k, f_k^* \rangle} \langle G(u_c + \Phi), f_k^* \rangle \\ &= \frac{1}{\langle f_k, f_k^* \rangle} \langle G_2(u_c, u_c) + G_2^s(u_c, \Phi) + G_3(u_c, u_c, u_c), f_k^* \rangle + O(4) \\ &:= P_{2,k} + P_{3,k} + O(4), \quad k = 1, 2 \end{aligned}$$

and (40) becomes

$$(41) \quad \frac{du_k}{dt} = \beta_k u_k + P_{2,k}(u_1, u_2) + P_{3,k}(u_1, u_2) + O(4), \quad k = 1, 2.$$

where $P_{2,k}(u_1, u_2)$ denote the quadratic terms in u_1, u_2 given by

$$\begin{aligned} P_{2,k} &= \frac{1}{\langle f_k, f_k^* \rangle} \langle G_2(u_c, u_c), f_k^* \rangle \\ &= \frac{1}{\langle f_k, f_k^* \rangle} \sum_{i,j=1}^2 \langle G_2(u_i f_i, u_j f_j), f_k^* \rangle \\ &= \sum_{i,j=1}^2 u_i u_j G_2(i, j, k), \quad k = 1, 2 \end{aligned}$$

and $P_{3,k}(u_1, u_2)$, $k = 1, 2$ denote the cubic terms given by

$$\begin{aligned} P_{3,k} &= \frac{1}{\langle f_k, f_k^* \rangle} \langle G_2^s(u_c, \Phi) + G_3(u_c, u_c, u_c), f_k^* \rangle \\ &= \frac{1}{\langle f_k, f_k^* \rangle} \sum_{i,l,m \in \{1,2\}, j \geq 3} \langle G_2^s(u_i f_i, \Phi_j f_j) + G_3(u_i f_i, u_m f_m, u_n f_n), f_k^* \rangle \\ &= \sum_{m,n \in \{1,2\}, j \geq 3} u_i u_m u_n \frac{-1}{\beta_j} G_2(m, n, j) G_2^s(i, j, k) \\ &\quad + \sum_{i,m,n \in \{1,2\}} u_i u_m u_n G_3(i, m, n, k) \end{aligned}$$

Now, we take into account the structure (3) of the eigenmodes into account.

4.2. Consequences of assumption on nonlinear operator. The condition (8) has the following implications.

$$(42) \quad (l_1, l_2) \notin C_{11} \implies \langle (G_2(e_{j_1, j_2}, e_{j_1, j_2}), e_{l_1, l_2}) \rangle = 0$$

$$(43) \quad (l_1, l_2) \notin C_{12} \implies \langle (G_2(e_{j_1, j_2}, e_{k_1, 0}), e_{l_1, l_2}) \rangle = 0$$

$$(44) \quad (l_1, l_2) \notin C_{12} \implies \langle (G_2(e_{k_1, 0}, e_{j_1, j_2}), e_{l_1, l_2}) \rangle = 0$$

$$(45) \quad (l_1, l_2) \notin C_{22} \implies \langle (G_2(e_{k_1, 0}, e_{k_1, 0}), e_{l_1, l_2}) \rangle = 0$$

where the index sets are as defined in (16).

Using the notation (10), the observations in (42)–(45) lead to the following observations

$$(46) \quad G_2(1, 1, 1) = G_2(2, 2, 1) = 0,$$

$$(47) \quad G_2(2, 2, 2) = G_2(2, 1, 2) = G_2(1, 2, 2) = 0.$$

But it is possible that

$$(48) \quad G_2(1, 2, 1) \neq 0, \quad G_2(2, 1, 1) \neq 0, \quad G_2(1, 1, 2) \neq 0$$

By (16), we note that

$$C_{11} \cap C_{12} = C_{12} \cap C_{22} = \emptyset$$

which implies that the following products of nonlinear interactions of the critical modes with higher modes vanish.

$$(49) \quad \begin{aligned} G_2(\sigma_1(1, 1, j))G_2(\sigma_2(1, 2, j)) &= 0, \quad \forall j \geq 3, \text{ since } C_{11} \cap C_{12} = \emptyset \\ G_2(\sigma_1(1, 2, j))G_2(\sigma_2(2, 2, j)) &= 0, \quad \forall j \geq 3, \text{ since } C_{12} \cap C_{22} = \emptyset \end{aligned}$$

where σ_1, σ_2 are any permutations of the set $\{1, 2, 3\}$. For example, the first condition above is equivalent to the vanishing of the 18 products given by

$$\begin{aligned} G_2(1, 1, j)G_2(1, 2, j) &= G_2(1, j, 1)G_2(1, 2, j) = G_2(j, 1, 1)G_2(1, 2, j) = 0, \\ G_2(1, 1, j)G_2(1, j, 2) &= G_2(1, j, 1)G_2(1, j, 2) = G_2(j, 1, 1)G_2(1, j, 2) = 0, \\ &\vdots \end{aligned}$$

and the same for the remaining 12 products as well for all $j \geq 3$.

Similarly, for the trilinear term, for $i, j, k, l \in \{1, 2\}$,

$$(50) \quad i + j + k + l = 1 \pmod{2} \implies G_3(i, j, k, l) = 0 \implies G_3^s(i, j, k, l) = 0.$$

4.3. Structure of the quadratic polynomials $P_{2,k}$. As a consequence of (47)

$$(51) \quad G_2^s(1, 2, 2) = G(1, 2, 2) + G(2, 1, 2) = 0.$$

Hence by (46), (47), and (51), the quadratic terms become

$$(52) \quad \begin{aligned} P_{2,1} &= u_1^2 G(1, 1, 1) + u_1 u_2 G_2^s(1, 2, 1) + u_2^2 G(2, 2, 1) \\ &= u_1 u_2 G_2^s(1, 2, 1) \end{aligned}$$

$$(53) \quad \begin{aligned} P_{2,2} &= u_1^2 G(1, 1, 2) + u_1 u_2 G_2^s(1, 2, 2) + u_2^2 G(2, 2, 2) \\ &= u_1^2 G(1, 1, 2) \end{aligned}$$

4.4. Structure of the cubic polynomials $P_{3,k}$. The coefficients of the following cubic terms vanish by (49) and (50).

(1) The term $u_1^2 u_2$ in $P_{3,1}$

$$\begin{aligned} G_3^s(1, 1, 2, 1) + \sum_{j \geq 3} \frac{-1}{\beta_j} (G(1, 2, j)G_2^s(1, j, 1) + G(2, 1, j)G_2^s(1, j, 1) \\ + G(1, 1, j)G_2^s(2, j, 1)) = 0, \end{aligned}$$

(2) The term u_2^3 in $P_{3,1}$

$$G_3(2, 2, 2, 1) + \sum_{j \geq 3} \frac{-1}{\beta_j} G(2, 2, j)G_2^s(2, j, 1) = 0,$$

(3) The term $u_1 u_2^2$ in $P_{3,2}$

$$\begin{aligned} G_3^s(1, 2, 2, 2) + \sum_{j \geq 3} \frac{-1}{\beta_j} (G(1, 2, j)G_2^s(2, j, 2) + G(2, 1, j)G_2^s(2, j, 2) \\ + G(2, 2, j)G_2^s(1, j, 2)) = 0, \end{aligned}$$

(4) The term u_1^3 in $P_{3,2}$

$$G_3(1, 1, 1, 2) + \sum_{j \geq 3} \frac{-1}{\beta_j} (G(1, 1, j)G_2^s(1, j, 2)) = 0,$$

4.5. The existence of bifurcated steady state solutions. We start by finding the straight line orbits of the vector field (F_1, F_2) given by (13) near $(u_1, u_2) = (0, 0)$. Clearly $u_1 = 0$ is always a straight line orbit that is $du_1/dt = 0$. On $u_1 = 0$, the dynamics of u_2 is as follows.

$$(54) \quad \frac{du_2}{dt} = u_2(\beta + b_3 u_2^2) + o(u_2^4).$$

For $\beta b_3 < 0$, we find the two bifurcated steady state solutions (roll pattern solutions) R_1, R_2 given by (17), that is with amplitudes $u_1 = 0$, and

$$(55) \quad u_1 = 0, \quad u_2 = \pm \sqrt{-\frac{\beta}{b_3}} + o(\sqrt{-\beta}).$$

Now we look for other straight line orbits $u_1 = k u_2$, $k \neq 0$ near the origin. On such a straight line orbit, the following relation is satisfied

$$k = \frac{u_1}{u_2} = \frac{F_1}{F_2} = \frac{a_1 k u_2^2 + O(u_2^3)}{b_1 k^2 u_2^2 + O(u_2^3)}, \quad u_2 \rightarrow 0.$$

Hence, for $k \neq 0$, k should satisfy the relation

$$k^2 b_1 = a_1.$$

In particular, if $a_1 b_1 < 0$, no such $k \neq 0$ exists.

On the other hand for $a_1 b_1 > 0$, in addition to $u_1 = 0$, four more straight line orbits appear

$$u_1 = k_i u_2, \quad k_i = (-1)^i \sqrt{a_1/b_1}, \quad i = 1, 2.$$

The flow on the straight line $u_1 = k_i u_2$ is given by

$$(56) \quad \frac{du_2}{dt} = u_2(\beta + b_1 k_i^2 u_2 + (b_2 k_i^2 + b_3) u_2^2),$$

which has two steady state solutions

$$(57) \quad \begin{aligned} u_1 = k_i u_2 &= (-1)^{i+1} \frac{\beta}{\sqrt{a_1 b_1}} + O(\beta^2), \\ u_2 &= -\frac{\beta}{b_1 k_i^2} + O(\beta^2) = -\frac{\beta}{a_1} + O(\beta^2), \quad i = 1, 2. \end{aligned}$$

On each line $u_1 = k_i u_2$, $i = 1, 2$, there is a bifurcated steady state solution which gives the amplitudes of (hexagonal pattern solution) H_1 and H_2 given by (18).

4.6. The stability of the bifurcated steady state solutions. The Jacobian matrix of the right hand side of the reduced equations (12) be

$$(58) \quad DF(u_1, u_2) = \begin{pmatrix} 3a_2u_1^2 + a_3u_2^2 + a_1u_2 + \beta & u_1(2a_3u_2 + a_1) \\ 2u_1(b_2u_2 + b_1) & b_2u_1^2 + 3b_3u_2^2 + \beta \end{pmatrix}.$$

Let us also denote the eigenvalues of DF by λ_1, λ_2 . We find that the eigenvalues of DF at the steady states (55) as below. For R_1 , that is for $(u_1, u_2) = (0, -\sqrt{-\frac{\beta}{b_3}}) + o(\sqrt{-\beta})$, they are

$$\lambda_1 = -2\beta, \quad \lambda_2 = -a_1\sqrt{-\frac{\beta}{b_3}} + O(\beta),$$

and for R_2 , that is for $(u_1, u_2) = (0, \sqrt{-\frac{\beta}{b_3}}) + o(\sqrt{-\beta})$, they are

$$\lambda_1 = -2\beta, \quad \lambda_2 = a_1\sqrt{-\frac{\beta}{b_3}} + O(\beta).$$

Thus the stability of the bifurcated solutions R_1, R_2 given by (17) for $\beta > 0$ are as follows.

$$\begin{aligned} a_1 > 0 & \quad R_1 \text{ is a stable node, } R_2 \text{ is a saddle} \\ a_1 < 0 & \quad R_1 \text{ is a saddle, } R_2 \text{ is a stable node} \end{aligned}$$

Since the amplitude (57) of the mixed mode steady states are $u_1 = (-1)^{i+1} \frac{\beta}{\sqrt{a_1 b_1}} + O(\beta^2)$, $u_2 = -\frac{\beta}{a_1} + O(\beta^2)$, we find that the Jacobian matrix of the mixed modes is

$$\begin{pmatrix} \beta + a_1 u_2 + O(\beta^2) & a_1 u_1 + O(\beta^2) \\ 2b_1 u_1 + O(\beta^2) & \beta + O(\beta^2) \end{pmatrix}$$

and the corresponding eigenvalues satisfy

$$\lambda_1 + \lambda_2 = \beta + O(\beta^2)$$

and

$$\lambda_1 \lambda_2 = -2a_1 b_1 u_1 u_2 + O(\beta^3) = -2\beta^2 + O(\beta^3)$$

Thus we find the eigenvalues and the corresponding eigenvectors of the amplitudes of the equilibria H_i as

$$H_1: \quad \lambda_1 = -\beta + O(\beta^2), v_1 = \begin{pmatrix} -\frac{a_1}{\sqrt{a_1 b_1}} \\ 1 \end{pmatrix}, \quad \lambda_2 = 2\beta + O(\beta^2), v_2 = \begin{pmatrix} \frac{a_1}{2\sqrt{a_1 b_1}} \\ 1 \end{pmatrix}$$

and

$$H_2: \quad \lambda_1 = -\beta + O(\beta^2), v_1 = \begin{pmatrix} \frac{a_1}{\sqrt{a_1 b_1}} \\ 1 \end{pmatrix}, \quad \lambda_2 = 2\beta + O(\beta^2), v_2 = \begin{pmatrix} -\frac{a_1}{2\sqrt{a_1 b_1}} \\ 1 \end{pmatrix}$$

Since the eigenvalues have always opposite signs near $\beta = 0$, the equilibria H_i given by (18) are always saddles whenever they exist.

The details of the proof of the main theorems follow from the above analysis and the dynamic transition theory [23, 22].

5. SUMMARY AND DISCUSSION

In this paper, we have found all possible transition scenarios of a general dissipative system with two dimensional critical center space. We have two main assumptions. First is the one that the one of the eigenmodes has a rectangle pattern and the other one has a roll pattern which is possible in spatial domains of at least two dimensions with homogeneous boundary conditions. The second one is an orthogonality condition on the nonlinear operator with respect to the basis vectors. This condition is generally satisfied when the bilinear and trilinear terms of the Taylor expansion of the nonlinear operator is a product of the unknown function and its derivatives.

Under the above general conditions, we manage to show that all three types of transitions of the dynamic transition theory are possible at the first criticality λ_c under generic conditions. We also determine the bifurcated steady state solutions with their stability and the bifurcated attractors in each case. Finally, we give several applications to demonstrate that all the conclusions of our main theorems are observable.

Up until now, the dynamic transition theory has been used as a general tool to understand specific problems. This paper points in the direction of determination of transitions and pattern formations for a general class of problems. Thus we believe that the results presented in this study will provide a general framework for the determination and the validity of transitions in many applications.

REFERENCES

- [1] Henri Bénard. Les tourbillons cellulaires dans une nappe liquide.-Méthodes optiques d'observation et d'enregistrement. *Journal de Physique Théorique et Appliquée*, 10(1):254–266, 1901.
- [2] Subrahmanyan Chandrasekhar. *Hydrodynamic and Hydromagnetic Stability*. The International Series of Monographs on Physics. Clarendon Press, Oxford, 1961.
- [3] Yuncherl Choi, Taeyoung Ha, Jongmin Han, and Doo Seok Lee. Bifurcation and final patterns of a modified Swift-Hohenberg equation. *Discrete & Continuous Dynamical Systems - B*, 22(7):2543–2567, 2017.
- [4] Pierre Colinet, Jean Claude Legros, and Manuel G. Velarde. *Nonlinear Dynamics of Surface-Tension-Driven Instabilities*. Wiley, first edition, May 2001.
- [5] M. C. Cross and P. C. Hohenberg. Pattern formation outside of equilibrium. *Reviews of Modern Physics*, 65(3):851–1112, July 1993.
- [6] Michael Cross and Henry Greenside. *Pattern Formation and Dynamics in Nonequilibrium Systems*. Cambridge University Press, 2009.

- [7] PC Dauby and G. Lebon. Bénard–Marangoni instability in rigid rectangular containers. *Journal of Fluid Mechanics*, 329(1):25–64, 1996.
- [8] PC Dauby, G. Lebon, P. Colinet, and J.C. Legros. Hexagonal Marangoni convection in a rectangular box with slippery walls. *The Quarterly Journal of Mechanics and Applied Mathematics*, 46(4):683, 1993.
- [9] H. A. Dijkstra. Pattern Selection in Surface Tension Driven Flows. In Hendrik C. Kuhlmann and Hans-Josef Rath, editors, *Free Surface Flows*, International Centre for Mechanical Sciences, pages 101–144, Vienna, 1998. Springer.
- [10] Henk Dijkstra, Taylan Sengul, and Shouhong Wang. Dynamic transitions of surface tension driven convection. *Physica D: Nonlinear Phenomena*, 247(1):7–17, March 2013.
- [11] Daozhi Han, Marco Hernandez, and Quan Wang. Dynamical transitions of a low-dimensional model for Rayleigh–Bénard convection under a vertical magnetic field. *Chaos, Solitons & Fractals*, 114:370–380, September 2018.
- [12] Daozhi Han, Marco Hernandez, and Quan Wang. Dynamic bifurcation and transition in the Rayleigh–Bénard convection with internal heating and varying gravity. *Communications in Mathematical Sciences*, 17(1):175–192, 2019.
- [13] Marco Hernández and Kiah Wah Ong. Stochastic Swift-Hohenberg Equation with degenerate linear multiplicative noise. *Journal of Mathematical Fluid Mechanics*, 20(3):1353–1372, September 2018.
- [14] Rebecca Hoyle. *Pattern Formation: An Introduction to Methods*. Cambridge University Press, Cambridge, 2006.
- [15] Chanh Kieu, Quan Wang, and Dongming Yan. Dynamical transitions of the quasi-periodic plasma model. *Nonlinear Dynamics*, 96(1):323–338, April 2019.
- [16] Yuri Kuznetsov. *Elements of Applied Bifurcation Theory*. Applied Mathematical Sciences. Springer-Verlag, New York, third edition, 2004.
- [17] Marcello Lappa. *Thermal Convection: Patterns, Evolution and Stability*. John Wiley & Sons, 2009.
- [18] Limei Li, Marco Hernandez, and Kiah Wah Ong. Stochastic attractor bifurcation for the two-dimensional Swift-Hohenberg equation. *Mathematical Methods in the Applied Sciences*, 41(5):2105–2118, March 2018.
- [19] Limei Li and Kiah Wah Ong. Dynamic Transitions of Generalized Burgers Equation. *Journal of Mathematical Fluid Mechanics*, 18(1):89–102, March 2016.
- [20] Honghu Liu, Taylan Sengul, Shouhong Wang, and Pingwen Zhang. Dynamic transitions and pattern formations for a Cahn–Hilliard model with long-range repulsive interactions. *Communications in Mathematical Sciences*, 13(5):1289–1315, 2015.
- [21] ChunHsien Lu, Yiqiu Mao, Quan Wang, and Dongming Yan. Hopf bifurcation and transition of three-dimensional wind-driven ocean circulation problem. *Journal of Differential Equations*, 267(4):2560–2593, August 2019.
- [22] Tian Ma and Shouhong Wang. *Bifurcation Theory and Applications*, volume 53 of *World Scientific Series on Nonlinear Science Series A*. World Scientific, June 2005.
- [23] Tian Ma and Shouhong Wang. *Phase Transition Dynamics*. Springer International Publishing, second edition, 2019.
- [24] J. D. Murray. *Mathematical Biology II: Spatial Models and Biomedical Applications*. Interdisciplinary Applied Mathematics, Mathematical Biology. Springer-Verlag, New York, third edition, 2003.
- [25] James D. Murray. *Mathematical Biology: I. An Introduction*. Interdisciplinary Applied Mathematics, Mathematical Biology. Springer-Verlag, New York, third edition, 2002.

- [26] Kiah Wah Ong. Dynamic transitions of generalized Kuramoto-Sivashinsky equation. *Discrete and Continuous Dynamical Systems - Series B*, 21(4):1225–1236, March 2016.
- [27] J. R. A. Pearson. On convection cells induced by surface tension. *Journal of Fluid Mechanics*, 4(5):489–500, September 1958.
- [28] Joseph Pedlosky. *Geophysical Fluid Dynamics*. Springer-Verlag, New York, second edition, 1987.
- [29] Lambertus A. Peletier and Vivi Rottschäfer. Pattern selection of solutions of the Swift–Hohenberg equation. *Physica D: Nonlinear Phenomena*, 194(1):95–126, July 2004.
- [30] S. Rosenblat, S. H. Davis, and G. M. Homsy. Nonlinear Marangoni convection in bounded layers. Part 1. Circular cylindrical containers. *Journal of Fluid Mechanics Digital Archive*, 120(-1):91–122, 1982.
- [31] S. Rosenblat, G. M. Homsy, and S. H. Davis. Nonlinear Marangoni convection in bounded layers. Part 2. Rectangular cylindrical containers. *Journal of Fluid Mechanics*, 120:123–138, July 1982.
- [32] Taylan Sengul, Jie Shen, and Shouhong Wang. Pattern formations of 2D Rayleigh–Bénard convection with no-slip boundary conditions for the velocity at the critical length scales. *Mathematical Methods in the Applied Sciences*, 38(17):3792–3806, November 2015.
- [33] Taylan Sengul and Shouhong Wang. Pattern formation in Rayleigh–Bénard convection. *Communications in Mathematical Sciences*, 11(1):315–343, 2013.
- [34] Taylan Sengul and Shouhong Wang. Pattern formation and dynamic transition for magnetohydrodynamic convection. *Communications on Pure and Applied Analysis*, 13(6):2609–2639, July 2014.
- [35] Martin B. Short, Andrea L. Bertozzi, and P. Jeffrey Brantingham. Nonlinear patterns in urban crime: Hotspots, bifurcations, and suppression. *SIAM Journal on Applied Dynamical Systems*, 9(2):462–483, 2010.
- [36] J. Swift and P. C. Hohenberg. Hydrodynamic fluctuations at the convective instability. *Physical Review A*, 15(1):319–328, January 1977.
- [37] Roger Temam. *Infinite-Dimensional Dynamical Systems in Mechanics and Physics*, volume 68 of *Applied Mathematical Sciences*. Springer-Verlag, New York, second edition, 1997.
- [38] Huichao Wang, Quan Wang, and Ruikuan Liu. A time-dependent perturbation solution from a steady state for Marangoni problem. *Applicable Analysis*, 97(9):1526–1539, July 2018.
- [39] Huichao Wang, Quan Wang, and Dongming Yan. On the stability and transition for the Navier-Stokes-alpha model. *Mathematical Methods in the Applied Sciences*, 43(5):2386–2402, 2020.
- [40] Quan Wang and Dongming Yan. On the stability and transition of the Cahn-Hilliard/Allen-Cahn system. *Discrete & Continuous Dynamical Systems - B*, 25(7):2607, 2020.
- [41] Xige Yang and Dapeng Li. Analyzing Turing’s Systems via Dynamic Bifurcation Theory. *arXiv:1811.10031 [math]*, November 2018.
- [42] Dongpei Zhang and Ruikuan Liu. Dynamical transition for S-K-T biological competing model with cross-diffusion. *Mathematical Methods in the Applied Sciences*, 41(12):4641–4658, August 2018.

DEPARTMENT OF MATHEMATICS, MARMARA UNIVERSITY, 34722 ISTANBUL, TURKEY

E-mail address: taylan.sengul@marmara.edu.tr